Materials Science and Engineering C 65 (2016) 393–399

Contents lists available at ScienceDirect

Materials Science and Engineering C

journal homepage: www.elsevier.com/locate/msec

In situ biosynthesis of bacterial nanocellulose-$CaCO_3$ hybrid bionanocomposite: One-step process

Faranak Mohammadkazemi [a,*], Marisa Faria [b], Nereida Cordeiro [b]

[a] Department of Cellulose and Paper Technology, Faculty of New Technologies Engineering, Shahid Beheshti University, Science and Research Campus, Zirab, Savadkooh, Mazandaran, Iran
[b] Faculty of Exact Science and Engineering, University of Madeira, Funchal, Portugal

ARTICLE INFO

Article history:
Received 30 December 2015
Received in revised form 14 March 2016
Accepted 18 April 2016
Available online 20 April 2016

Keywords:
Bacterial nanocellulose
Gluconacetobacter xylinus
Hybrid bio-nanocomposites
$CaCO_3$
In situ biosynthesis

ABSTRACT

In this work, a simple and green route to the synthesis of the bacterial nanocellulose-calcium carbonate (BNC/$CaCO_3$) hybrid bionanocomposites using one-step *in situ* biosynthesis was studied. The $CaCO_3$ was incorporated in the bacterial nanocellulose structure during the cellulose biosynthesis by *Gluconacetobacter xylinus* PTCC 1734 bacteria. Hestrin-Schramm (HS) and Zhou (Z) culture media were used to the hybrid bionanocomposites production and the effect of ethanol addition was investigated. Attenuated total reflection Fourier transform infrared spectroscopy, field emission scanning electron microscopy, X-ray diffraction, energy-dispersive X-ray spectroscopy, inverse gas chromatography and thermogravimetric analysis were used to characterize the samples. The experimental results demonstrated that the ethanol and culture medium play an important role in the BNC/$CaCO_3$ hybrid bionanocomposites production, structure and properties. The BNC/$CaCO_3$ biosynthesized in Z culture medium revealed higher O/C ratio and amphoteric surface character, which justify the highest $CaCO_3$ content incorporation. The $CaCO_3$ was incorporated into the cellulosic matrix decreasing the bacterial nanocellulose crystallinity. This work reveals the high potential of *in situ* biosynthesis of BNC/$CaCO_3$ hybrid bionanocomposites and opens a new way to the high value-added applications of bacterial nanocellulose.

1. Introduction

Recently, the organic/inorganic (hybrid) bionanocomposites have offered a diversity of interesting applications in different fields of activity, from industry to medicine due to their remarkable properties such as biocompatibility, biodegradability and for being environmentally friendly [1,2]. Such properties arises from synergy effects between them and can be found in nature, over long time, in bones, corals, pearls, mollusk shells, eggshells and exoskeleton of arthropods [2].

Bacterial nanocellulose (BNC) is a natural and extracellular biopolymer synthesized like nanofibrils at the air-liquid culture medium interface forming a three-dimensional network by Gram-negative acetic bacteria *Gluconacetobacter xylinus*, one of the best bacterial species and the most efficient producer for the production of BNC in large-scale [3,4]. BNC is biocompatible, biodegradable, chemically pure (free of undesirable components such as lignin and hemicellulose), highly crystalline, with high water retention capacity (99%) and degree of polymerization that distinguishes it from other forms of cellulose [5,6]. This biopolymer has high potential for the development of a new class of truly green bionanocomposites as a reinforcement material due to its high young's modulus; which can be up to 134 GPa [7]. Many studies have reported the potential of BNC as reinforcement in bionanocomposites for biomedical devices, wound healing and tissue regeneration, medicine, food production, textile industry, mining and refinery, broadcasting, forestry, paper industry, machine industry, and transparent films [8–13].

Calcium phosphate, hydroxyapatite, calcium silicate, calcium carbonate and calcium sulfate are some calcium-based inorganic nanomaterials employed in biomedical fields [14]. Calcium carbonate ($CaCO_3$) as one of the main inorganic components of human bone, shells and teeth is known to have biological activity with protein-adhesive properties, cell compatibility and hard tissue compatibility, and is the major biomineral present in some organisms [1,15,16]. $CaCO_3$-BNC bionanocomposite would be a suitable candidate both as implants in the tissue engineering of artificial skin, blood vessels, bones, cartilage, would healing and drug delivery [2,17].

BNC is an ecological sustainable biopolymer and due to its reticulated nanofibrous structure can be a suitable matrix for obtaining different types of calcium carbonate crystals with enhanced biocompatibility [18]. BNC, as a substrate favoring the deposition of calcite crystals in different conditions, could control the crystallization process and modify the polymorphs of $CaCO_3$ crystals [16,19]. Additionally, it was found that the interfacial bonding strength between the BNC and $CaCO_3$ was good for effective hydrogen bond and physical entanglement, and makes the bacterial nanocellulose-$CaCO_3$ bionanocomposite to have high young's modulus [18,20]. In recent papers, ultrasonic irradiation [17], impregnation [18] and microwave [2] are some techniques used to modify the deposition of $CaCO_3$ crystals in the BNC network. The

* Corresponding author.
E-mail address: f_mkazemi@sbu.ac.ir (F. Mohammadkazemi).

http://dx.doi.org/10.1016/j.msec.2016.04.069
0928-4931/

merit of this method, as compared with other techniques, is the ease of process and excellent interaction between components. In the other words, $CaCO_3$ particles would be adhered to the reticulated fibrils during production of BNC without additional cost or any further post processing. This study aimed at deposition of $CaCO_3$ crystals on BNC network *in situ* during BNC biosynthesis to produce hybrid bionanocomposites and investigation of the surface interaction and structural properties.

This research develops a green strategy for the synthesis of BNC/$CaCO_3$ hybrid bionanocomposites without solvents, in only one-step process. The BNC/$CaCO_3$ hybrid bionanocomposite was formed *in situ* during BNC synthesis from a local bacterial strain of *G. xylinus* PTCC (Persian Type Culture Collection) 1734.

The effect of culture medium, ethanol and $CaCO_3$ addition on the BNC production was explored. The changes in the morphological structure, chemical composition, crystallinity, thermal stability and surface properties of BNC were determined by field emission scanning electron scanning electron microscopy (FE-SEM), attenuated total reflection Fourier transform infrared spectroscopy (ATR-FTIR), energy-dispersive X-ray spectroscopy (EDX), X-ray diffraction (XRD), thermogravimetric analysis (TGA) and inverse gas chromatography (IGC).

2. Experimental

2.1. Biosynthesis of bacterial nanocellulose-$CaCO_3$ hybrid bionanocomposites

The organism used for the production of cellulose in this work was a strain of *G. xylinus* obtained from the Persian Type Culture Collection (PTCC), strain number 1734. The strain was cultured on glucose yeast extract (GYE) agar containing 100 g D-glucose, 10 g yeast extract, 5 g peptone, 20 g $CaCO_3$, 25 g agar per liter. After three days of being cultured in 28 °C, 50 mL pre-culture medium composed of Hestrin-Schramm (HS) culture medium, in 250 mL Erlenmeyer flasks was autoclaved at 121 °C for 15 min before inoculation. Then, the flasks were cooled to room temperature and inoculated with the stock culture (10% v/v) and incubated in a shaker (150 rpm and 28 °C). Then, Hestrin-Schramm (HS) and Zhou (Z) culture media containing glucose as a carbon source (Table 1), with ethanol (1% v/v) and $CaCO_3$ (2% w/v) were cultured in 250 mL baffled shaker flasks (three v-shaped Notches or indentations in the sides of flasks). All media were cultured at 80 rpm and 28 °C for 7 days. After the incubation period, harvested cellulose membrane was washed with 1% NaOH at 80 °C for 1 h and then washed with distilled water repeatedly until a neutral pH was reached. The bacterial nanocellulose-$CaCO_3$ membrane (BNC/$CaCO_3$) obtained were named by HS-BNC/$CaCO_3$ and Z-BNC/$CaCO_3$.

A control system consisting of pure bacterial nanocellulose in $CaCO_3$ absence was biosynthesized following the same methodology described for BNC/$CaCO_3$ in $CaCO_3$ free culture media. The samples were named by HS-BNC and Z-BNC.

To study the effect of ethanol addition, bacterial nanocellulose was biosynthesized following the same methodology described for BNC/$CaCO_3$, but in a culture medium without ethanol and $CaCO_3$. The samples were named by HS-BNC/AEt and Z-BNC/AEt.

To determine the dry weight, biosynthesized BNCs were oven dried at 45 °C for three days and then weighed. The dry weight of BNC within the volume of culture medium in liter (g/L) was calculated. The results presented are the average values.

Table 1
Components and concentrations of culture media (%, w/v).

Components	Hestrin-Schramm (HS)	Zhou (Z)
Glucose	2	4
Corn steep liquor (CSL)	–	2
Yeast extract	0.5	–
Peptone	0.5	–
Na_2HPO_4	0.27	–
Citric acid. H_2O	0.115	–
$(NH_4)_2SO_4$	–	0.4
KH_2PO_4	–	0.2
$MgSO_4 \cdot 7H_2O$	–	0.04

2.2. Attenuated total reflection Fourier transform infrared spectrometry (ATR-FTIR)

Before analysis the samples were properly dried at 40 °C to remove moisture. ATR-FTIR spectra were recorded on a Bruker spectrophotometer in the 4000–600 cm^{-1} range using attenuated total reflection. The spectra were recorded with a resolution of 5 cm^{-1} and an accumulation of 16 scans.

2.3. Field emission scanning electron microscopy (FE-SEM), energy-dispersive X-ray spectroscopy (EDX)

The samples surface morphology and structure were investigated using a field emission scanning electron microscope (FE-SEM, Hitachi SU 8090). The samples were mounted and gold-coated in preparation for FE-SEM. Identification of chemical compositions of samples and semi-quantitative analysis were carried out by energy-dispersive X-ray spectroscopy (EDX). Quantitative analyses were done for weight percentages (wt.%) of elements and the O/C ratio was obtained. Both FE-SEM and EDX experiments were conducted at an accelerated voltage of 5 kV.

2.4. X-ray diffraction (XRD)

XRD pattern of BNC was collected in order to measure the crystallinity and crystallite size of BNC on X'Pert pro MPD (multi-purpose diffractometer, Model PW3040/60) with CuKα radiation generation at a temperature of 25 °C, resolution of 0.001°, voltage of 40 kV, and filament emission of 40 mA. Diffraction intensities were measured between 2θ of 5–50°. The crystallinity (Cr) and crystallite size (CrS) were calculated based on X-ray diffraction measurements. Crystallinity was calculated from the following Eq.:

$$Cr(\%) = S_c/S_t \times 100 \quad (1)$$

where S_c is sum of net the area and S_t is sum of the total area. The CrS was determined using Scherrer equation as following:

$$CrS = K\lambda/\beta\cos\theta \quad (2)$$

where K is the shape factor (0.9), λ is the x-ray wavelength (1.54 Å), β is the full width at half maximum height (FWHM), and θ is the Bragg's angle.

2.5. Thermogravimetric analysis (TGA)

Thermogravimetric analysis of samples were done using a TGA instrument 931 thermal analyzer (TA Instruments). The samples weight was approximately 0.8 mg. Scan rates of 20 °C min^{-1} over a temperature range of 40–550 °C were applied. All tests were carried out under inert (N_2) atmosphere.

2.6. Inverse gas chromatography (IGC)

IGC measurements were carried out using a commercial Inverse gas chromatography (Surface Measurements Systems, London, UK) equipped with flame ionization (FID) and thermal conductivity (TCD) detectors. The data obtained were analyzed in *i*GC Standard v1.3 and Advanced Analysis Software v1.21 [21].

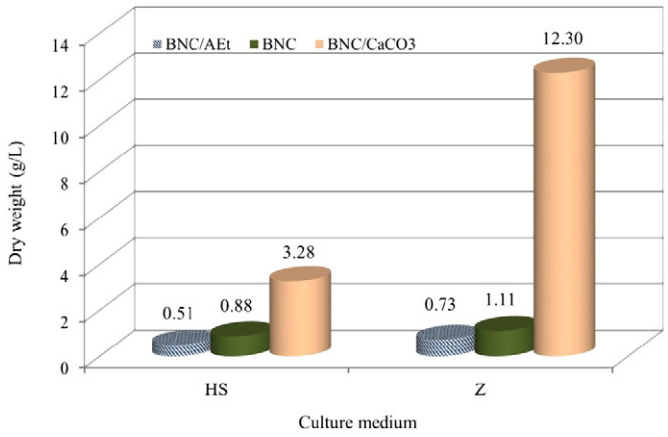

Fig. 1. Dry weigh (g/L) of bacterial nanocellulose biosynthesized in Hestrin-Schramm (HS) and Zhou (Z) culture medium, with (BNC) and without ethanol (BNC/AEt), and bacterial nanocellulose-$CaCO_3$ hybrid bionanocomposite (BNC/$CaCO_3$).

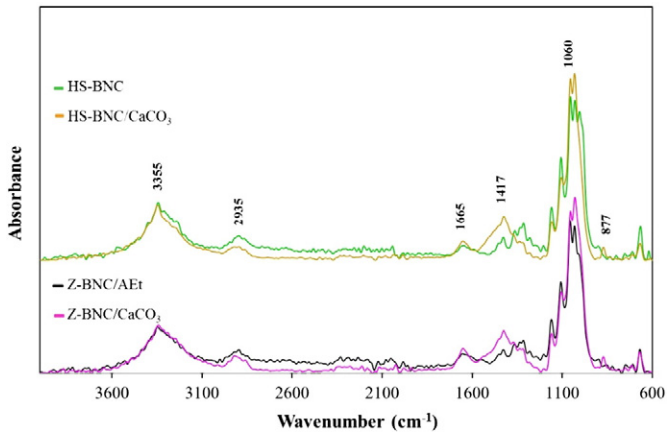

Fig. 3. ATR-FTIR spectra of the bacterial nanocellulose biosynthesized in Hestrin-Schramm (HS) and Zhou culture medium (Z) and bacterial cellulose-$CaCO_3$ hybrid bionanocomposite (HS-BNC/$CaCO_3$ and Z-BNC/$CaCO_3$).

To study the dispersive surface interactions a series of *n*-alkanes (heptane, octane, nonane and decane) were used. For acid-base studies, tetrahydrofuran, ethanol, ethyl acetate and acetonitrile were used at the same conditions than that used for dispersive surface interaction measurements. The isotherms were determined with different concentrations of *n*-octane, ethanol and tetrahydrofuran. All measurements were carried out at 0% relative humidity, at 25 °C and a flow with a rate of 10 mL min^{-1}. Methane was used as the reference molecule for calculating the dead time. The experiments were performed in duplicate and the presented results are the average values. The experimental error due to the temperature variation, flow rate and retention time measurement was estimated to be below 4%.

3. Results and discussion

3.1. Bacterial nanocellulose-$CaCO_3$ hybrid bionanocomposites production

With the aim to study the media effect in the bacterial nanocellulose (BNC) production two culture media were used: Hestrin-Schramm (HS) and Zhou (Z). The BNC dry weight biosynthesized in the Z culture medium was higher (26%) than in the HS culture medium (Fig. 1).

It is observed that at the end of BNC production the pH of the HS culture medium was higher (3.56) than the Z culture medium (2.24). This indicates that the HS culture medium had higher resistance to pH change than the Z culture medium, however Z culture medium has the highest production. The main component of the Z culture medium is the corn steep liquor (CSL) that was reported as a rich nitrogen source, having a stimulating effect on bacterial cellulose production [22].

The literature show a positive influence of ethanol on BNC production, by enhancing the ATP (Adenosine-5-triphosphate) content of viable cells and degenerating of the cellulose non-producing cells of bacteria [23,24,25,26,27]. Following this goal, the ethanol effect in the BNC production was also studied. The dry weight of BNCs biosynthesized in HS and Z culture media containing ethanol were increased 73% and 52% (Fig. 1), respectively in comparison to the media without ethanol. As the ethanol addition highly influence the BNC production, the bacterial nanocellulose-$CaCO_3$ (BNC/$CaCO_3$) hybrid bionanocomposites production was carried out in medium with ethanol. The dry weights of BNC/$CaCO_3$ hybrid bionanocomposites were 4 and 11 times more than those for BNC in HS and Z culture medium, respectively (Fig. 1). This remarkable increase can be due to: (*i*) the $CaCO_3$ incorporation in the BNC network; (*ii*) the $CaCO_3$ effect in the BNC production. $CaCO_3$ can act as a buffer that keeps the pH of culture medium constant and higher than 4, value below which BNC production usually stop [28]. As the pH decreased more in the Z culture medium than in the HS culture medium, this effect has more relevance, and can explain the large increase in the production in Z culture medium; (*iii*) the baffled flasks break effect. The presence of baffles in the flask can improve the efficiency of oxygen transfer since they increase the turbulence when the medium is agitated on a shaker [29]. Baffled flasks force aeration and help in the mixing of medium components, cells, and oxygen.

In the Z culture medium, the BNC/$CaCO_3$ hybrid bionanocomposites production present a value 275% higher than that with HS culture medium. Therefore, it is thought that the culture medium played an important role in the BNC/$CaCO_3$ hybrid bionanocomposites production by the *G. xylinus* PTCC 1734 bacteria.

Fig. 2. Shape of bacterial nanocellulose-$CaCO_3$ hybrid bionanocomposites biosynthesized in Z culture medium containing $CaCO_3$ (2% w/v) in a baffled shaker flasks; (a) unwashed; (b) washed.

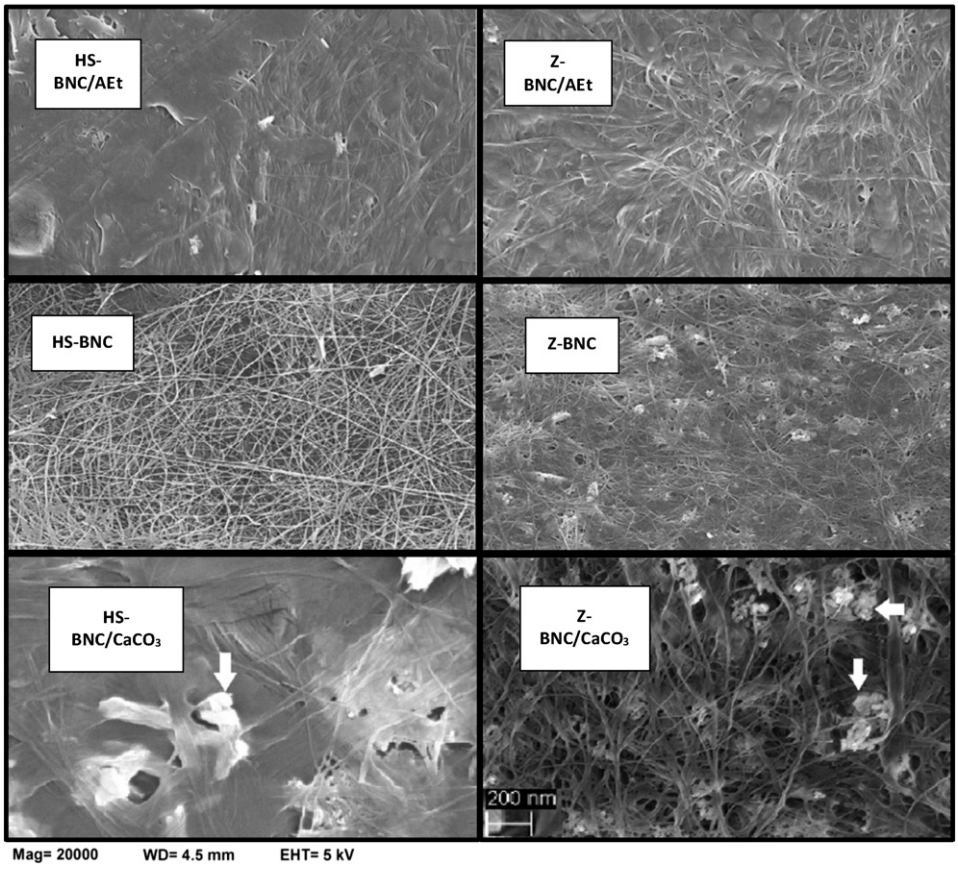

Fig. 4. FE-SEM micrographs of bacterial nanocellulose biosynthesized in Hestrin-Schramm (HS) and Zhou culture medium (Z), with (HS-BNC and Z-BNC) and without ethanol (HS-BNC/AEt and Z-BNC/AEt), and bacterial nanocellulose-$CaCO_3$ hybrid bionanocomposite (HS-BNC/$CaCO_3$ and Z-BNC/$CaCO_3$). The arrows indicate $CaCO_3$ particles dispersed in bacterial nanocellulose matrix.

3.2. Bacterial nanocellulose-$CaCO_3$ hybrid bionanocomposites characterization

As can be observed in Fig. 2, a large mass of BNC/$CaCO_3$ hybrid bionanocomposites with a continuous structure which filled the bottom of the flask was biosynthesized in the baffled shaker flask.

The ATR-FTIR spectra of the biosynthesized BNC are shown in Fig. 3. The absorption bands at 3355, 2935, 1665, 1370, 1164, and 1060 cm^{-1} typically associated with BNC were found. Moreover, a strong absorption band at 1417 cm^{-1} and a medium intensity band at 877 cm^{-1} in the spectra, attributed to calcite (the most stable polymorph of $CaCO_3$) [2], provide indication of the successfully $CaCO_3$ incorporation in the BNC network.

The morphologies of the BNC and BNC/$CaCO_3$ were investigated by FE-SEM (Fig. 4). All the BNCs presented the typical three-dimensional network structure of random nanofiber with the diameter between 31 and 41 nm, which provides an excellent scaffold to $CaCO_3$ nanoparticles incorporation. Compacted BNC ribbons were formed given rise to a dense BNC and interweaved structure which revealed a strong interfacial adhesion between BNC fibers. The FE-SEM micrographs of the BNC/$CaCO_3$ using HS and Z culture medium show the presence of calcium carbonate crystals (marked by arrows) dispersed in the three-dimensional network of BNC microfibrils, evidence of the hybrid bionanocomposite formation.

The XRD patterns for pure BNC and the BNC/$CaCO_3$ hybrid bionanocomposites synthesized are given in Fig. 5. BNCs present typical

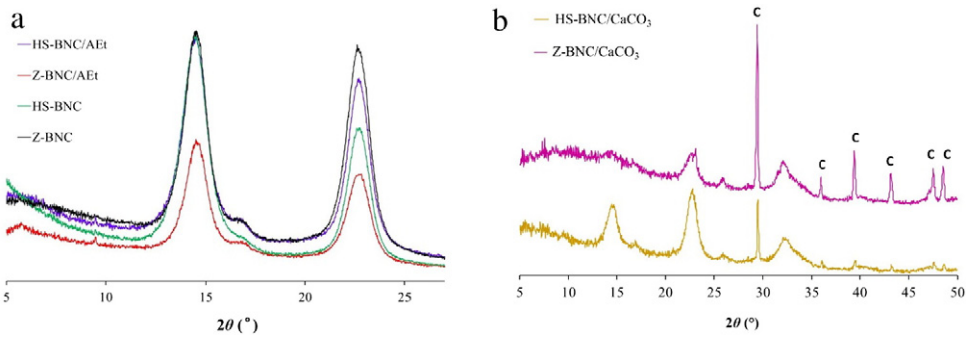

Fig. 5. X-ray diffractograms of (a) bacterial nanocellulose biosynthesized in Hestrin-Schramm (HS) and Zhou (Z) culture medium, with (HS-BNC and Z-BNC) and without ethanol (HS-BNC/AEt and Z-BNC/AEt), and (b) bacterial nanocellulose-$CaCO_3$ hybrid bionanocomposite (HS-BNC/$CaCO_3$ and Z-BNC/$CaCO_3$).

Table 2
Crystallinity (%) of BNC biosynthesized in Hestrin-Schramm (HS) and Zhou (Z) culture medium.

Samples	Crystallinity (%)
Hestrin-Schramm culture medium	
HS-BNC/AEt	65
HS-BNC	76
HS-BNC/$CaCO_3$	38
Zhou culture medium	
Z-BNC/AEt	56
Z-BNC	62
Z-BNC/$CaCO_3$	31

diffraction pattern of cellulose type I ($22° \le 2\theta \le 23°$), with the main diffraction peaks at $2\theta = 14.7°$, 17.0° and 22.8°, assigned to the diffraction planes (101), (10$\bar{1}$) and (002), respectively (Fig. 5a). The relative peak intensity decreased drastically in BNC biosynthesis with $CaCO_3$ (Fig. 5b). This means that the incorporated $CaCO_3$ lead to a decrease of the crystallinity of the bacterial nanocellulose. Besides, extra peaks located at $2\theta = 29.4°$, 36.0°, 39.4°, 43.2°, 47.5°and 48.5° appear. These peaks were attributed to characteristic peaks of $CaCO_3$ crystals [15,30], which confirm that the $CaCO_3$ were successfully incorporated in BNC matrix.

The degree of crystallinity was calculated (Table 2) and the results reveal that the BNC harvested in HS culture medium had higher degree of crystallinity. Also, an increase in the degree of crystallinity when ethanol was added to the culture medium was observed. As previously suggested by the XRD patterns, the crystallinity degree decreased significantly (50%) when $CaCO_3$ was added to the biosynthesis process.

The elemental composition of the samples was analyzed by EDX and is resumed in Table 3. As expected, carbon (C) and oxygen (O) were the dominant elements detected in all samples. The O/C ratios of BNC harvested from the media containing ethanol were higher than those without ethanol, indicating that the addition of ethanol to culture medium plays an important role in the structure of the BNC, given rise to carboxyl enriched BNC surface. These higher O/C ratios increase the reactive sites and promote the increase in $CaCO_3$ content, as previously observed with other carboxyl group enriched polymers [31].

The chemical composition of the BNC/$CaCO_3$ surface was also examined and the presence of $CaCO_3$ was evidenced by the calcium (Ca) detection. It is observed that calcium particles are well distributed throughout the BNC/$CaCO_3$ surface. The EDX results show that the percentage of calcium, and thus the amount of $CaCO_3$, present at the surface of Z-BNC/$CaCO_3$ is higher than at the surface of HS-BNC/$CaCO_3$ (Table 3).

With the aim to identify the interaction mechanism between $CaCO_3$ and BNC, responsible to the $CaCO_3$ incorporation in the bacterial nanocellulose, and explain why BNC biosynthesized in Z culture medium incorporate more $CaCO_3$, the inverse gas chromatography (IGC) technique was used. IGC measurements allow to know the surface properties including the acid-base characteristics. This knowledge enables us to know their compatibility and behavior with other molecules.

Through non-polar and polar probes molecules the dispersive component of surface energy (γ_s^d) and the specific component of surface energy (ΔG_S^{sp}) were determined, respectively. Table 4 resume the obtained IGC results. The γ_s^d found for the BNCs is in the range of those reported in the literature for bacterial nanocelluloses [4]. The BNC obtained from the Z culture medium presented a more dispersive surface (more 15%) when compared to the BNC obtained from H culture medium.

Table 3
EDX analysis of elemental composition of bacterial nanocellulose samples (wt.%).

Samples	C	O	Ca	O/C	O/Ca
HS-BNC/AEt	62.37	33.51	–	0.54	–
Z-BNC/AEt	59.17	38.16	–	0.64	–
HS-BNC	59.88	37.06	–	0.62	–
Z-BNC	53.65	39.22	–	0.73	–
HS-BNC/$CaCO_3$	36.35	44.50	8.23	1.22	4.42
Z-BNC/$CaCO_3$	30.97	41.83	11.62	1.35	3.60

Table 4
Dispersive component of the surface energy (γ_s^d) and acid and base constants (K_a and K_b) of the bacterial nanocellulose biosynthesized in Hestrin-Schramm (HS-BNC) and Zhou culture medium (Z-BNC).

IGC data	HS-BNC	Z-BNC
($mJ.m^{-2}$)	37.08	42.55
K_a	0.09	0.09
K_b	0.06	0.09
K_a/K_b	1.50	1.00

The polar groups in the BNCs surface are able to exchange specific interactions with polar molecules and could be studied by the ΔG_S^{sp}. Thus, ΔG_S^{sp}.was determined by IGC by applying four polar probes: tetrahydrofuran (THF), ethanol (EtOH), ethyl acetate (EtAc) and acetonitrile (AcN). The most significant differences were observed for ethanol (acid probe) and acetonitrile (amphoteric probe), as can be seen in Fig. 6.

Acetonitrile displays a stronger interaction with the BNC harvested in Z culture medium, indicating more polar groups in the Z-BNC surface, which was in agree with the higher oxygen content found in this BNC. The higher ΔG_S^{sp} found to ethanol in the Z-BNC indicate a more basic surface character. The energy profile obtained from the ethanol (Fig. 7a) supports this observation, where Z-BNC present more number of active sites and with higher energy than in HS-BNC surface. On the other hand, the THF (basic probe) profile (Fig. 7b) shows that the HS-BNC surface presents more acid groups (OH) relatively to the Z-BNC surface.

The obtained values of were converted into acid-base constants (K_a and K_b) using the Gutmann's concept [32]. The results (Table 4) allow the conclusion that HS-BNC has an acid surface (K_a/K_b ratio of 1.50) and Z-BNC has an amphoteric surface (K_a/K_b ratio of 1).

Thus, these results show that the higher $CaCO_3$ incorporation take place preferentially in an amphoteric BNC surface.

The thermal stability of the BNC and BNC/$CaCO_3$ hybrid bionanocomposites were also investigated by TGA. TGA degradation curves of the dried BNCs are shown in Fig. 8. A small weight loss starting at room temperature up to 200 °C was observed. This is due to the loss of the water physically absorbed and no differences were beholden between BNC samples in this region. The second, but not the end mass loss, takes place between 280 and 400 °C, and is attributed to thermal degradation/depolymerization of BNC [33]. In this region, decomposition of BNC ended at 400 °C, except for BNC biosynthesized in HS culture medium with ethanol (ended at 380 °C). Thermal degradation behavior is known to be affected by some structural parameters such

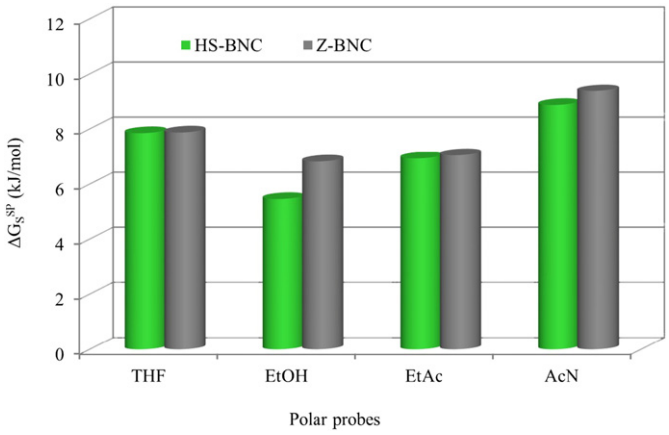

Fig. 6. Specific surface free energy (ΔG_S^{sp}), obtained for bacterial nanocellulose biosynthesized in Hestrin-Schramm (HS-BNC) and Zhou (Z-BNC) culture medium with ethanol.

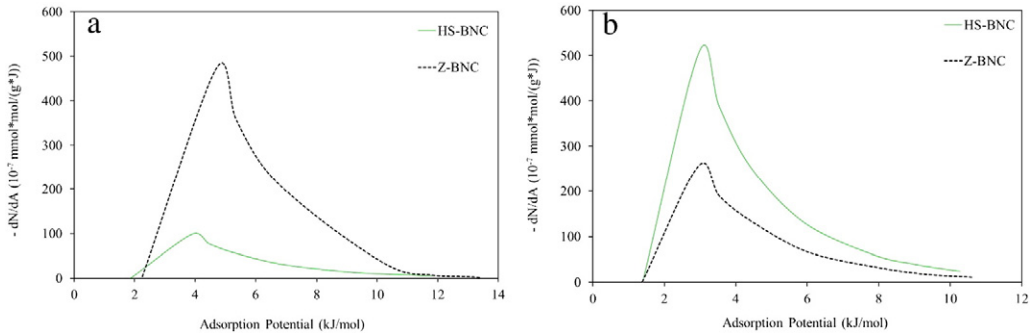

Fig. 7. Energetic profiles obtained with ethanol (a) and tetrahydrofuran (b) onto bacterial nanocellulose surface biosynthesized in Hestrin-Schramm (HS-BNC) and Zhou (Z-BNC) culture medium with ethanol.

as molecular weight, crystallinity, and orientation of the fibers [34,35]. According to XRD analysis (Table 2), BNC harvested from HS culture medium with ethanol had the highest crystallinity, which could be the reason for the thermal behavior difference observed.

The end mass loss is seen from 400 to 550 °C and is assigned to decomposition of glucose units and formation of an inorganic residue. In pure BNC, the inorganic residues are in the range 25–31% at 550 °C. However, the BNC/$CaCO_3$ hybrid bionanocomposites presented a residue up to 57%, confirming $CaCO_3$ incorporation on the BNC matrix. $CaCO_3$ content in the hybrid bionanocomposites could be calculated as the difference between the residue from pure ethanol BNC and BNC/$CaCO_3$ hybrid bionanocomposites. Taking this into account, values of 26% and 49% were found to BNC/$CaCO_3$ harvested from HS and Z media, respectively, confirming that the production in Z culture medium allowed the incorporation of more $CaCO_3$ in the BNC matrix.

4. Conclusions

In this work, a one-step process to synthesize bacterial nanocellulose-$CaCO_3$ hybrid bionanocomposite is reported for the first time. The results demonstrate that the bacterial nanocellulose synthetized by *Gluconacetobacter xylinus* PTCC 1734 strain bacteria was favored in Z culture medium containing ethanol. Furthermore, the hybrid bionanocomposites biosynthesized in Z culture medium show higher $CaCO_3$ content incorporation. The $CaCO_3$ particles are preferential retained in the matrix with high O/C ratio and with amphoteric surface character. The particles were homogeneously dispersed in the cellulose matrix and the original crystalline structure of BNC was disrupted in the hybrid bionanocomposites formation. Hence, the results proved the successfully synthesis of the bacterial nanocellulose-$CaCO_3$ hybrid bionanocomposite and that this new methodology can be used to obtain new product for a widespread number of applications, as in the biomedical field to obtain scaffolds for bone regeneration.

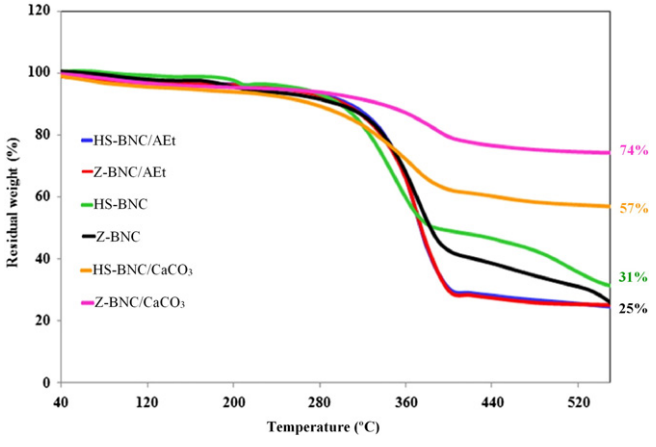

Fig. 8. TGA curves of the bacterial nanocellulose biosynthesized in Hestrin-Schramm (HS) and Zhou culture medium (Z), with (HS-BNC and Z-BNC) and without ethanol (HS-BNC/AEt and Z-BNC/AEt), and bacterial nanocellulose-$CaCO_3$ hybrid bionanocomposite (HS-BNC/$CaCO_3$ and Z-BNC/$CaCO_3$). % of pyrolysis residue at 550 °C presented next the TGA curves.

Acknowledgement

This work was supported by the grant from credit research of Shahid Beheshti University G.C. The contract number is 600/2107.

References

[1] N. Jia, S.M. Li, M.G. Ma, R.C. Sun, J.F. Zhu, Hydrothermal fabrication, characterization, and biological activity of cellulose/$CaCO_3$ bionanocomposites, Carbohydr. Polym. 88 (2012) 179–184.
[2] A. Stoica-Guzun, M. Stroescu, S.I. Jinga, I.M. Jipa, T. Dobre, Microwave assisted synthesis of bacterial cellulose-calcium carbonate bionanocomposites, Ind. Crop. Prod. 50 (2013) 414–422.
[3] S. Bielecki, A. Krystynowicz, M. Turkiewicz, H. Kalinowska, Bacterial Cellulose, Wiley-VCH, Germany, 2001.
[4] C. Castro, N. Cordeiro, M. Faria, R. Zuluaga, J.L. Putaux, I. Filpponen, L. Velez, O.J. Rojas, P. Gañán, In-situ glyoxalization during biosynthesis in bacterial cellulose, Carbohydr. Polym. 126 (2015) 32–39.
[5] M. Moosavi-Nasab, A.R. Yousefi, Biotechnological production of cellulose by *Gluconacetobacter xylinus* from agricultural waste, Iran. J. Biotechnol. 9 (2011) 94–101.
[6] S. Saska, H.S. Barud, A.M.M. Gaspar, R. Marchetto, S.J.L. Ribeiro, Y. Messaddeq, Bacterial cellulose-hydroxyapatite Nanobiocomposites for bone regeneration, Int. J. Biomater. 2011 (2011), http://dx.doi.org/10.1155/2011/175362.
[7] D. Klemm, D. Schumann, F. Kramer, N. Hessler, M. Hornung, H.P. Schmauder, S. Marsch, Nanocelluloses as innovative polymers in research and application, Adv. Polym. Sci. 205 (2006) 49–96.
[8] C. Castro, R. Zuluaga, J.L. Putaux, G. Caro, I. Mondragon, P. Ganan, Structural characterization of bacterial cellulose produced by gluconacetobacter swingsii sp. from Colombian agroindustrial wastes, Carbohydr. Polym. 84 (2011) 96–102.
[9] A.N. Nakagaito, S. Iwamoto, H. Yano, Bacterial cellulose: the ultimate nano-scalar cellulose morphology for the production of high-strength bionanocomposites, Appl. Phys. A Mater. Sci. Process. 80 (2005) 93–97.
[10] H. Yano, J. Sugiyama, A.N. Nakagaito, M. Nogi, T. Matsuura, M. Hikita, K. Handa, Optically transparent bionanocomposites reinforced with networks of bacterial nanofibers, Adv. Mater. 17 (2005) 153–155.
[11] H. Meada, M. Nakajima, T. Hagiwara, T. Sawaguchi, S. Yano, Bacterial cellulose/silica hybrid fabricated by mimicking bionanocomposites, J. Mater. Sci. 41 (2006) 5646–5656.
[12] C.J. Grande, F.G. Torres, C.M. Gomez, O.P. Tonocoso, J. Canet-Ferrer, J. Martinez-Pastor, Morphological characterization of bacterial cellulose-starch bionanocomposites, Polym. Polym. Compos. 16 (2008) 181–185.
[13] Y.Z. Wan, H. Luo, F. He, H. Liang, Y. Huang, X.L. Li, Mechanical, moisture absorption, and biodegradation behaviors of bacterial cellulose fiber-reinforced starch bionanocomposites, Compos. Sci. Technol. 69 (2009) 1212–1217.
[14] M.G. Ma, J.F. Zhu, Recent progress on fabrication of calcium-based inorganic biodegradable nanomaterials, Recent Pat. Nanotechnol. 4 (2010) 164–170.
[15] M.G. Ma, Y.Y. Dong, L.H. Fu, S.M. Li, R.C. Sun, Cellulose/$CaCO_3$ bionanocomposites: microwave ionic liquid synthesis, characterization, and biological activity, Carbohydr. Polym. 92 (2013) 1669–1676.
[16] C. Vilela, C.S.R. Freire, P.A.A.P. Marques, T. Trindade, C.P. Neto, Synthesis and characterization of new $CaCO_3$/cellulose bionanocomposites prepared by controlled hydrolysis of dimethylcarbonate, Carbohydr. Polym. 79 (2010) 1150–1156.

[17] P.T. Sudheesh Kumar, C. Ramya, R. Jayakumar, S.k.V. Nair, V.-K. Lakshmanan, Drug delivery and tissue engineering applications of biocompatible pectin–chitin/nano $CaCO_3$ composite scaffolds, Colloids Surf. B Biointerfaces 106 (2013) 109–116.
[18] A. Stoica-Guzun, M. Stroescu, S.I. Jinga, I.M. Jipa, T. Dobre, Ultrasound influence upon calcium carbonate precipitation on bacterial cellulose membranes, Ultrason. Sonochem. 19 (2012) 909–915.
[19] F.G. Torres, S. Commeaux, O.P. Troncoso, Biocompatibility of bacterial cellulose-based biomaterials, J. Funct. Biomater. 3 (2012) 864–878.
[20] G. Serafica, R. Mormino, H. Bungay, Inclusion of solid particles in bacterial cellulose, Appl. Microbiol. Biotechnol. 58 (2002) 756–760.
[21] N. Cordeiro, C. Gouveia, A.G.O. Moraes, S.C. Amico, Natural fibers characterization by inverse gas chromatography, Carbohydr. Polym. 84 (2011) 110–117.
[22] N. Noro, M. Sugano, M. Shoda, Utilization of the buffering capacity of corn steep liquor in bacterial cellulose production by Acetobacter xylinum, Appl. Microbiol. Biotechnol. 64 (2004) 199–205.
[23] H.J. Son, H.G. Kim, K.K. Kim, H.S. Kim, Y.G. Kim, S.J. Lee, Increased production of bacterial cellulose by Acetobacter sp. V6 in synthetic media under shaking culture conditions, Bioresour. Technol. 86 (2003) 215–219.
[24] J.K. Park, J.Y. Jung, Y.H. Park, Cellulose production by gluconacetobacter hansenii in a medium containing ethanol, Biotechnol. Lett. 25 (2003) 2055–2059.
[25] P.R. Chawla, I.B. Bajaj, S.A. Survase, R.S. Singhal, Microbial cellulose: fermentative production and applications, Food Technol. Biotechnol. 47 (2009) 107–124.
[26] M. Matsuoka, T. Tsuchida, K. Matsishita, O. Adachi, F. Yoshinaga, A synthetic medium for bacterial cellulose production by Acetobacter xylinum subsp. Sucrofermentans, Biosci. Biotechnol. Biochem. 60 (1996) 575–579.
[27] J.K. Park, Y.H. Park, J.Y. Jung, Production of bacterial cellulose by gluconacetobacter hansenif PJK isolated from rotten apple, Biotechnol. Bioprocess Eng. 8 (2003) 83–88.
[28] M.A. Rivadeneyra, I. Perez-Garcia, V. Salmeron, A. Ramos-Cormenzana, Bacterial precipitation of calcium carbonate in presence of phosphate, Soil Biol. Biochem. 17 (1985) 171–172.
[29] A.J. Nair, Introduction to Biotechnology and Genetic Engineering: Microbial Culture and Applications, Infinity Science Press LLC, Massachusetts/New Delhi, India, 2008.
[30] M.G. Ma, L.H. Fu, R.C. Sun, N. Jia, Compared study on the cellulose/$CaCO_3$ bionanocomposites via microwave-assisted method using different cellulose types, Carbohydr. Polym. 90 (2012) 309–315.
[31] E. Dousi, J. Kallitis, A. Chrissanthopoulos, A.H. Mangood, E. Dalas, Calcite overgrowth on carboxylated polymers, J. Cryst. Growth 253 (2003) 496–503.
[32] V. Gutmann, The Donor–Acceptor Approach to Molecular Interactions, NY Plenum Publ. Corp, New York, 1978.
[33] A. Vazquez, M.L. Foresti, P. Cerruti, M. Galvagno, Bacterial cellulose from simple and low cost production media by *Gluconacetobacter xylinus*, J. Polym. Environ. 21 (2013) 545–554.
[34] F. Mohammadkazemi, K. Doosthoseini, M. Azin, Effect of ethanol and medium on bacterial cellulose (BC) production by *Gluconacetobacter xylinus* (PTCC 1734), Cellul. Chem. Technol. 49 (5–6) (2015) 455–462.
[35] H.S. Barud, C.A. Ribeiro, M.S. Crespi, M.A.U. Martines, J. Dexpert-Ghys, R.F.C. Marques, Y. Messaddeq, S.J.L. Ribeiro, Thermal characterization of bacterial cellulose-phosphate bionanocomposite membranes, J. Therm. Anal. Calorim. 87 (2007) 815–818.